N-glycan microheterogeneity regulates interactions of plasma proteins

Di Wu[a], Weston B. Struwe[a,b], David J. Harvey[c], Michael A. J. Ferguson[d], and Carol V. Robinson[a,1]

[a]Department of Chemistry, University of Oxford, Oxford OX1 3QZ, United Kingdom; [b]Department of Biochemistry, Oxford Glycobiology Institute, University of Oxford, Oxford OX1 3QU, United Kingdom; [c]Target Discovery Institute, Nuffield Department of Medicine, University of Oxford, Oxford OX3 7FZ, United Kingdom; and [d]Wellcome Centre for Anti-Infectives Research, School of Life Sciences, University of Dundee, Dundee DD1 5EH, United Kingdom

Altered glycosylation patterns of plasma proteins are associated with autoimmune disorders and pathogenesis of various cancers. Elucidating glycoprotein microheterogeneity and relating subtle changes in the glycan structural repertoire to changes in protein–protein, or protein–small molecule interactions, remains a significant challenge in glycobiology. Here, we apply mass spectrometry-based approaches to elucidate the global and site-specific microheterogeneity of two plasma proteins: α1-acid glycoprotein (AGP) and haptoglobin (Hp). We then determine the dissociation constants of the anticoagulant warfarin to different AGP glycoforms and reveal how subtle N-glycan differences, namely, increased antennae branching and terminal fucosylation, reduce drug-binding affinity. Conversely, similar analysis of the haptoglobin–hemoglobin (Hp–Hb) complex reveals the contrary effects of fucosylation and N-glycan branching on Hp–Hb interactions. Taken together, our results not only elucidate how glycoprotein microheterogeneity regulates protein–drug/protein interactions but also inform the pharmacokinetics of plasma proteins, many of which are drug targets, and whose glycosylation status changes in various disease states.

glycoprotein | mass spectrometry | protein interactions

Glycosylation is one of the most common and complex post-translation modifications that influences the structural and functional properties of proteins (1–3). N-linked glycans are covalently linked to asparagine (Asn) residues during protein translation. They are biosynthesized and processed by a series of glycosyltransferases and glycohydrolases in a non–template-directed manner, giving rise to heterogeneous glycoforms that impact protein folding, stability, protein–protein interactions, and cell–cell recognition (2, 3). The subtle variations in glycan structure are regulated by primary amino acid sequence, as well as quaternary structure and the repertoire of processing enzymes alongside the Golgi apparatus transit times in the glycoprotein-producing cells (4). Changes in glycosylation are associated with many diseases and play direct roles in pathological processes, including cancer metastasis, diabetes, and inflammation (5, 6). Moreover, the efficacy of a number of biotherapeutics, such as cytokines, hormones, Fc-fusion proteins, and monoclonal antibodies, are known to be affected by their glycosylation status (7). It is crucial therefore to elucidate functional properties of individual glycan structures and relate site-specific glycosylation to ligand or drug interactions.

Due to the complexity of glycoproteins and the limitations of existing analytical methodologies, the distribution of glycans on a protein glycosylation site, commonly known as its microheterogeneity, and their impact on protein–ligand/drug binding is not fully understood. Current lectin-array and mass spectrometry (MS)-based glycomics approaches target the collective pool of enzymatic or chemically released glycans from all sites simultaneously. As a result, these approaches do not define the site of specific glycan structures. Other methods to study glycoprotein interactions, namely, isothermal titration calorimetry, surface plasmon resonance, and analytical ultracentrifugation, lack detailed affinity information for individual glycoproteoforms (8). Methods to produce homogeneous glycoproteins are available, including exoglycosidase

digestion or expression in glycosyltransferase-engineered cell lines, but these glycoprotein products typically differ from the "wild-type" form and therefore preclude functional studies of biologically relevant glycosylation.

The recent emergence of high-resolution native MS represents a tool for glycobiology capable of measuring both glycan composition and glycosylation site occupancy of intact glycoproteins (9–11). Supplemented by established liquid chromatography (LC)-MS/MS–based glycoproteomics methods, native MS enables a comprehensive understanding of protein glycosylation and is capable of revealing over 200 glycoproteoforms on a single glycoprotein (12). In parallel to these developments in glycobiology, high-resolution native MS has been developed to measure protein–drug interactions quantitatively and to analyze variable drug affinities for different proteoforms (13, 14), but not previously for glycoproteoforms. Here, we describe the development and application of an approach to investigate glycoprotein interactions between drugs and proteins using two plasma proteins: α1-acid glycoprotein (AGP) and haptoglobin (Hp). We focus, first, on elucidating their structural microheterogeneity and, second, on how this heterogeneity impacts drug or protein binding.

The high-abundance acute-phase plasma protein AGP is a main carrier of many endogenous hormones, lipids, and exogenous drugs,

Significance

Glycosylation is one of the most common and complex post-translation modifications that significantly influences protein structure and function. However, linking individual glycan structures to protein interactions remains challenging and typically requires multiple techniques. Here, we establish a mass-spectrometric approach to systematically dissect the microheterogeneity of two important serum proteins, α1-acid glycoprotein and haptoglobin, and relate glycan features to drug and protein-binding interaction kinetics. We found that the degree of N-glycan branching and extent of terminal fucosylation can attenuate or enhance these interactions, providing important insight into drug transport in plasma. Our study demonstrates an approach capable of investigating how protein glycosylation fine-tunes protein–drug interactions at the glycan-specific level and will prove universally useful for studying glycoprotein interactions.

CHEMISTRY

BIOCHEMISTRY

and is proposed to deliver bound drugs to cells by conformational changes induced by the cell membrane (15). These drug-binding mechanisms are complicated, however, since AGP carries five highly sialylated and branched complex type N-glycans (15, 16). Two N-glycans at Asn38 and Asn75 border the entrance to the primary drug-binding site of AGP, a hydrophobic cavity about 9–12 Å, revealed by X-ray crystallography of the recombinant nonglycosylated protein (17, 18). There is evidence for a correlation between aberrant AGP glycosylation and altered drug-binding capacity, but as yet there is no molecular detail of this modulation (19–21).

A second high-abundance acute-phase plasma glycoprotein, Hp, clears free hemoglobin (Hb) from lysed erythrocytes, eliminating Hb-induced oxidative stress and recycling iron in tissues and the body (22). It consists of two nonglycosylated α-subunits (Hp α) and two heavily glycosylated β-subunits (Hp β) cross-linked by disulfide bonds. Hp β-subunits mediate the binding of the Hp–Hb complex to the scavenger receptor CD163, facilitating the endocytosis of the complex by macrophages (23). It is reported that a small fraction of human Hp, which binds weakly to Hb, exhibits an altered glycosylation pattern (24). How glycoprotein microheterogeneity of Hp modulates its affinity for Hb through N-glycosylation, however, is unclear.

Here, we develop and apply high-resolution native MS and LC-MS–based glycoproteomics methods to first define the global and site-specific microheterogeneity of AGP and Hp. Using a common anticoagulant drug (warfarin) that binds to the hydrophobic cavity of AGP with a dissociation constant of 4 μM (25, 26), we then correlate changes in drug-binding kinetics to specific glycan structures. We then contrast and compare these results with a quantitative analysis of the effects of Hp glycosylation on Hp–Hb interactions.

Results

MS Analysis Reveals the Complex Microheterogeneity of AGP.
AGP is known to have five glycosites occupied by complex type N-glycans with multiple antennary α1–3-linked fucose and N-acetylneuraminic acid (Neu5Ac) residues forming sialyl Lewis^X epitopes on Asn15, Asn38, Asn54, Asn75, and Asn85 (Fig. 1A) (16, 27, 28). AGP F1 and S variants are the most common proteoforms with 1-aa difference (F1, Gln-20, and S, Arg-20) (29–31). The native MS spectrum of sialylated AGP is highly complex due to the varying degree of sialylation across all sites (*SI Appendix*, Fig. S1). Importantly, the mass of two fucose residues (292.29 Da) and one Neu5Ac (291.26 Da) are similar and cannot be resolved on the intact protein by native MS (32). Therefore, assignment of the glycan composition of the highly heterogeneous sialylated AGP is ambiguous in terms of fucosylation and sialylation. We selected asialo-AGP (neuraminidase-treated AGP) for the following experiments to reduce the complexity of the spectrum and to improve our assignments.
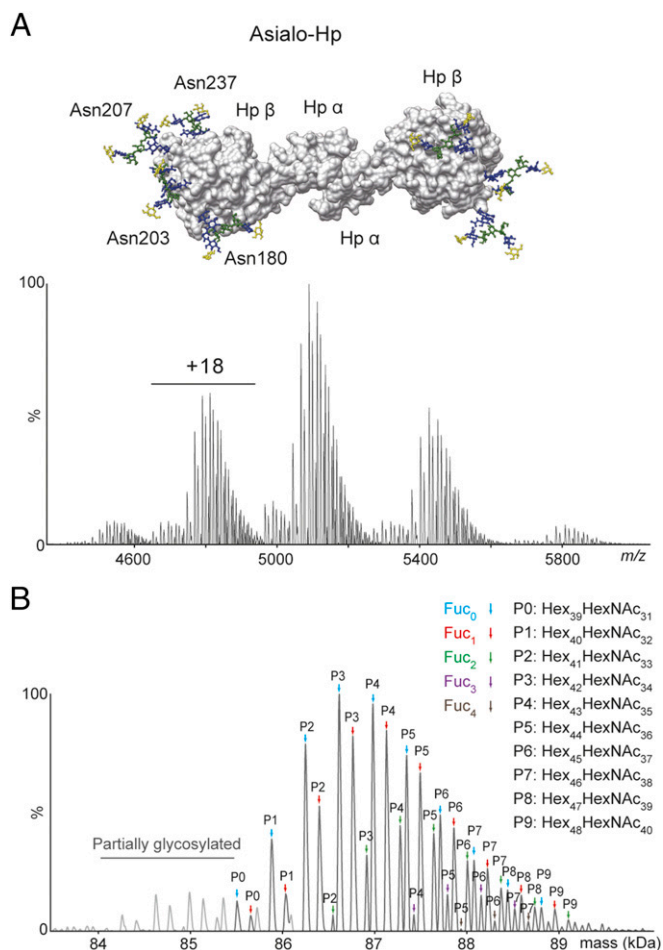
The native mass spectrum of asialo-AGP shows a peak envelope from m/z 2,900–4,300 with reduced spectral complexity compared with the sialylated form (Fig. 1A). After deconvolution by UniDec software (33), the base peak (32,213 Da) was assigned as $Hex_{32}HexNAc_{27}Fuc_0$, which is within 1 Da of the theoretical glycoprotein mass [AGP F1 variant peptide backbone, 21,539.06; $Hex_{32}HexNAc_{27}Fuc_0$ residue mass, 10,674.82 Da; Hex for mannose (Man) and galactose (Gal); HexNAc for N-acetylglucosamine (GlcNAc), Fuc for fucose] (Fig. 1B). N-glycosylation is established as the only posttranslational modification on AGP accounting for this heterogeneity (15). Two series of peak were identified with a 28-Da mass difference, corresponding to the known AGP F1 and S variants (Fig. 1B, blue and yellow peaks). The other peaks in the mass spectrum were assigned to the corresponding glycoproteoforms based on mass differences of 146.1430 Da (Fuc_1) for fucosylation and 365.3374 Da ($Hex_1HexNAc_1$) for N-glycan branching and elongation (Fig. 1B). We found that N-glycan branching and fucosylation could account for all observed AGP glycan
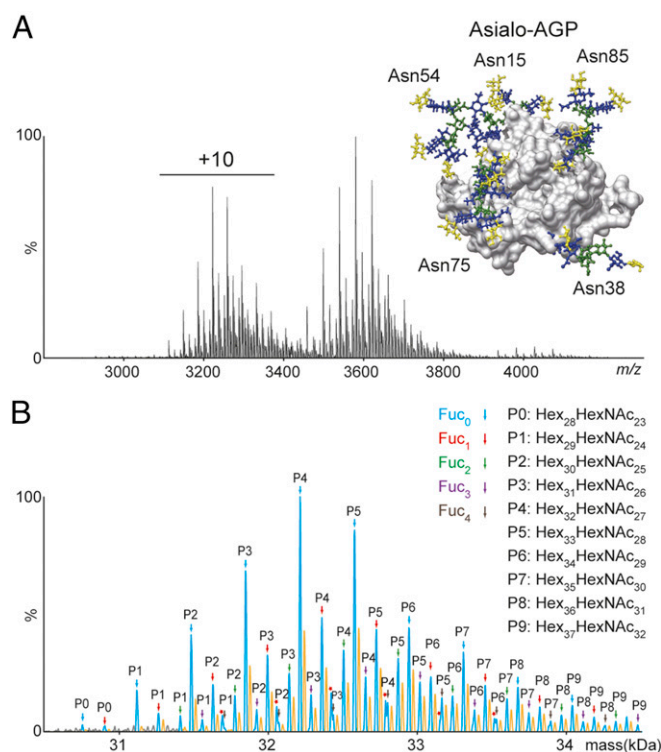
Fig. 1. Native MS analysis of asialo-AGP. (A) Native mass spectrum of asialo-AGP. AGP structure with five highly branched N-glycans at Asn15, Asn38, Asn54, Asn75, and Asn85 are shown. The monosaccharide residues are labeled according to the Consortium for Functional Glycomics guidance (blue for GlcNAc, yellow for Gal, and green for Man). (B) A zero-charged native mass spectrum of asialo-AGP is constructed using UniDec. Each peak is assigned to the corresponding glycan composition (*SI Appendix*, Table S1). Peaks with the same hexose (Hex) and N-acetylhexosamine (HexNAc) numbers are labeled P0 to P9. The number of fucose residues assigned to each peak (Fuc_0 to Fuc_4) is denoted with colored arrows. The presence of an "uncapped" GlcNAc residue on AGP is denoted with a red asterisk (*). This may arise either from incomplete processing of AGP, escaping from the N-glycosylation biosynthesis pathway, or from degradation AGP in vivo and/or in vitro.

heterogeneity and were consistent with the 10 main peak series with $Hex_1HexNAc_1$ differences (marked P0 to P9 in Fig. 1B). Each peak series contains five glycoproteoforms ranging from unfucosylated to tetrafucosylated (Fuc_0 to Fuc_4, Fig. 1B). Importantly, the difference in mass between five fucose residues (730.715 Da) and $Hex_2HexNAc_2$ (730.6748 Da) is 0.0402 Da. Therefore, we cannot rule out the presence of low-abundance highly fucosylated AGP carrying five or more fucose residues that overlap with other peaks in the native mass spectra. However, given this caveat, from the baseline-resolved peaks and applying a 5-Da mass tolerance, we were able to identify over 90 glycoproteoforms (Fig. 1B and *SI Appendix*, Table S1). We also evaluated the site-specific microheterogeneity of asialo-AGP by glycoproteomics and glycomics (*SI Appendix*, Figs. S2 and S3), and revealed that the glycan composition and relative abundance of N-glycan branching/elongation on each N-glycosylation site are in agreement with previous reports (16, 28). Importantly, Neu5Ac residue was not detected by either glycoproteomics or glycomics analysis, suggesting that the neuraminidase reaction went to completion and confirming the native MS assignment of asialo-AGP (Fig. 1B).

Native MS Analysis Resolves the Microheterogeneity of Hp.
The human plasma Hp has a genetic polymorphism expressed by two alleles HP1 and HP2, resulting in three major phenotypes: Hp1-1, Hp2-1, and Hp2-2 (34). Here, we selected the simplest form

Fig. 2. Resolving the microheterogeneity of asialo-Hp. (*A*) Native mass spectrum of asialo-Hp. Hp structure with four biantennary N-glycans at Asn180, Asn203, Asn207, and Asn237 at each Hp β-subunit is shown. (*B*) A zero-charged native mass spectrum of asialo-Hp. Each peak is assigned to the corresponding glycan composition (*SI Appendix*, Table S2). Peaks with the same Hex and HexNAc numbers are labeled P0 to P9. The number of fucose residues assigned to each peak (Fuc$_0$ to Fuc$_4$) is denoted with colored arrows.

Hp1-1 consisting of two α1 (9.1 kDa) and two glycosylated β-subunits (40 kDa) for native MS analysis. Each β-subunit has four highly sialylated complex type N-glycans with antennary α1–3-linked and/or core α1–6-linked fucose on Asn180, Asn203, Asn207, and Asn237 (Fig. 2*A*) (35, 36). The native MS spectrum of Hp shows a peak envelope from *m/z* 4,600–6,300 with partially overlapping charge states (*SI Appendix*, Fig. S4). The asialo-Hp native mass spectrum exhibits significantly reduced complexity with less overlapping charge states (Fig. 2*B*). The glycan composition of the base peak (86,615 Da) was assigned as Hex$_{42}$HexNAc$_{34}$Fuc$_0$ within 0.1 Da of the theoretical mass of 86,615.08 Da (Hp protein backbone, 72,896.47 Da; Hex$_{42}$HexNAc$_{34}$Fuc$_0$ residue mass, 13,718.61 Da) (P3 form in Fig. 2*B*). Other peaks were assigned to the corresponding glycoproteoforms based on mass differences of 146.1430 Da (Fuc$_1$) for fucosylation and 365.3374 Da (Hex$_1$HexNAc$_1$) for N-glycan branching and elongation (*SI Appendix*, Table S2). Notably, the glycan composition of the P0 form (Hex$_{39}$HexNAc$_{31}$) suggests the presence of one monoantennary and seven biantennary N-glycans on Hp. We also found the presence of partially glycosylated Hp which has seven N-glycans (Fig. 2*B* and *SI Appendix*, Table S2). The N-glycan occupancy at N237 gives rise to this heterogeneity at the glycoprotein level (37). The glycoproteomics analysis of asialo-Hp revealed biantennary and triantennary N-glycans are predominantly distributed on all four glycosylation sites (*SI Appendix*, Fig. S5). We also detected the presence of monoantennary N-glycan on Asn237, supporting the native MS assignment of asialo-Hp (Fig. 2*B*).

Comparing the results for Hp to those of AGP shows higher sialylation, and less fucosylation and N-glycan branching on Hp. Because the labile Neu5Ac residues are not stable in glycoproteomics analysis (38) and largely complicate the native mass spectrum, we selected asialo-Hp and asialo-AGP for the following experiments to reduce the complexity of the spectrum and to improve the assignment.

N-glycan Branching and Fucosylation Reduce the Affinity of Asialo-AGP to Warfarin. N-glycans can function to stabilize glycoprotein structures and also decrease glycoprotein dynamics (39). Due to their inherent flexibility and heterogeneity, the influence of N-glycosylation on protein–drug interactions is complex and in most cases not fully understood. To explore asialo-AGP interactions with drugs, we selected warfarin, a well-known anticoagulant plasma protein drug for which in-solution studies have shown stoichiometric binding to AGP (25). First, we examined asialo-AGP with an excess of warfarin, ~1 μM asialo-AGP and 50 μM warfarin in 200 mM ammonium acetate and 1% dimethyl sulfoxide (DMSO). Noncovalent interactions between asialo-AGP and warfarin were maintained in the gas phase with warfarin binding to each glycoproteoform (+308.33 Da) clearly observed (Fig. 3*A*). Charge state reduction was also apparent in the mass spectrum due to the effect of low levels of DMSO (40). Interestingly, we found that asialo-AGP bound warfarin with 1:1 stoichiometry without any nonspecific binding detected in a 50-fold excess of warfarin (Fig. 3*A*).

Next, we measured the affinity of asialo-AGP binding to warfarin through titration of increasing concentrations of the drug in 200 mM ammonium acetate and 1% DMSO. Peaks assigned to unfucosylated and monofucosylated glycoproteoforms bound to warfarin were clearly resolved with high signal-to-noise ratios. The relative abundance of nonfucosylated and monofucosylated peaks as a function of drug concentration were extracted and normalized by UniDec software (33) and fit to a single-site specific binding model for dissociation constant (K_d) calculations. The K_d of warfarin binding to 16 unfucosylated and monofucosylated glycoproteoforms (identified as P1 to P8) ranged from 200 to 500 nM (Fig. 3*B*) and are in broad agreement with the average value obtained via in-solution measurements (K_d of 4 μM) (25). Importantly, we found that fucosylation significantly reduces the affinity of asialo-AGP to warfarin. Similarly, N-glycan branching/elongation also decreases asialo-AGP binding to warfarin (Fig. 3*C*).

It is notable that fucosylation has a greater influence on inhibiting AGP binding to warfarin than N-glycan branching/elongation, despite the fact that addition of a single fucose residue (146 Da) is less than the addition of Hex$_1$HexNAc$_1$ unit (365 Da). This implies that, for inhibition of warfarin binding to asialo-AGP, the size of the additional monosaccharide residue is not as important as the steric hindrance of the species as a result of the position of the linkage of the monosaccharide residue. It is likely that fucosylation and N-glycan branching/elongation introduces steric hindrance to warfarin by preventing access to the drug-binding cavity (Fig. 3*D*). Previously, an inverse relationship between AGP drug-binding capacity and GlcNAc/Man ratio has been reported (20, 21). Our results directly show that N-glycan branching (Hex$_1$HexNAc$_1$) and fucosylation (Fuc$_1$) attenuate the AGP affinity to the drug. We rationalize this finding by providing K_d measurements for individual drug-binding events for defined glycoproteoforms. In this way, we have been able to assign functional properties to discrete complex N-glycans on the surface of AGP (see Fig. 5).

Fucosylation and N-glycan Branching Regulates Hp Interactions to Hb. To explore the impact of glycosylation on protein–protein interaction, we quantitatively studied the high-affinity interaction
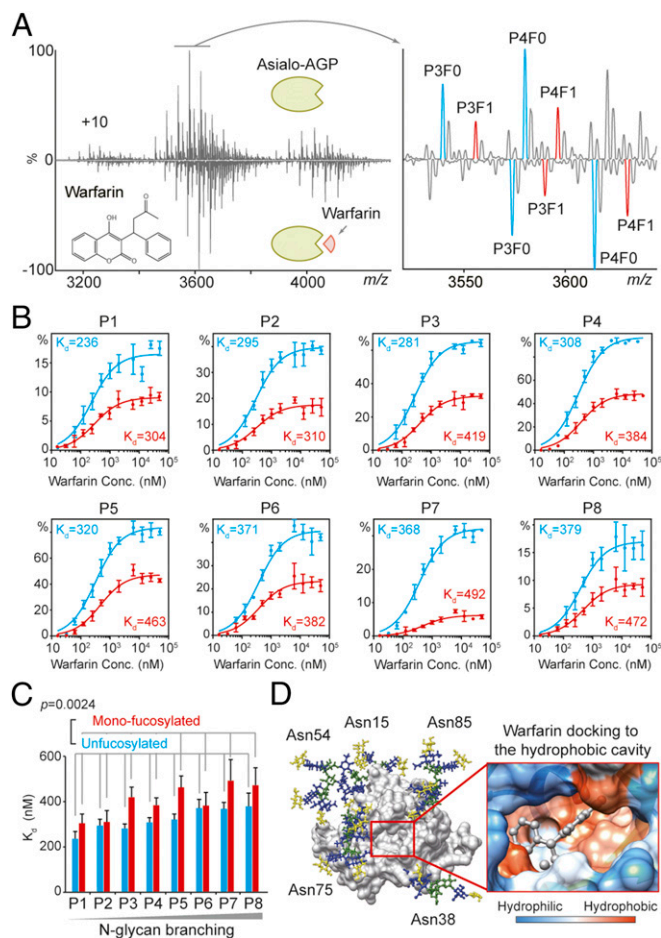
Fig. 3. Native MS analysis of asialo-AGP and warfarin binding. (*A*) Native mass spectra of asialo-AGP in 1% DMSO and asialo-AGP with 50 μM warfarin in 1% DMSO. Warfarin binding to asialo-AGP results in a mass shift of 308.33 Da. Unfucosylated P3F0/P4F0 and monofucosylated P3F1/P4F1 are labeled as blue and red peaks, respectively. Warfarin-bound asialo-AGP peaks do not overlap with *apo*-asialo-AGP peaks. (*B*) Plots of the warfarin concentration to the relative abundances of warfarin-bound unfucosylated (P1F0 to P8F0) and monofucosylated (P1F1 to P8F1) glycoproteoforms. The abundance of each peak was normalized to the total abundance of P4F0 form (P4F0 unbound and bound peaks). Dissociation constants for each glycoproteoform were calculated by a one-site specific binding model. Error bars represent the SE of three replicate experiments. (*C*) Bar graph of dissociation constants of unfucosylated (P1 to P8) and monofucosylated (P1 to P8) glycoproteoforms show that fucosylation and N-glycan branching elevate dissociation constant of asialo-AGP to warfarin. (*D*) AGP structure with warfarin docking to the hydrophobic cavity. N-glycans on Asn38 and Asn75 are close to the hydrophobic cavity for drug binding.

of human asialo-Hp and the human Hb heterodimer (Fig. 4*A*) (41, 42). First, we analyzed asialo-Hp by native MS and calculated the relative abundances of unfucosylated and monofucosylated peak series of fully glycosylated Hp (eight N-glycans) with high signal-to-noise ratios (P1 to P7, Fig. 4*B*). Then we analyzed the Hp–Hb complex by native MS, which is formed from two Hb holo-heterodimers (theoretical mass, 32,226.56 Da) binding to one Hp heterotetramer (Fig. 4*C* and *SI Appendix*, Fig. S6). To minimize the gas-phase unfolding of the Hp–Hb complex, we applied minimal source energy (50 V) to desolvate the complex and to resolve unfucosylated, monofucosylated, and fully glycosylated Hp–Hb complexes (P1 to P7, Fig. 4*C*). We quantified the relative abundances of unfucosylated and monofucosylated peak series and compared their abundances to the corresponding glycoproteoforms in Hp alone (Fig. 4*D*). Interestingly, fucosylation significantly

stabilizes the Hp–Hb complex. By contrast, N-glycan branching reduces the affinity of Hp for Hb.

These results imply that the fucose residue on Hp interacts with Hb to stabilize the Hp–Hb complex and/or alter the orientation of N-glycan antennae to rectify the steric hindrance of the branched N-glycans. Notably, monofucosylation on Hp can rescue the negative effects of N-glycan branching on the Hp–Hb interaction (P1 unfucosylated and P6 monofucosylated; Fig. 4*D*). Multifucosylation on Hp largely increases its affinity for Hb (*SI Appendix*, Fig. S7). We also captured dissociated Hp–Hb complex, formed by loss of one holo-Hb β-subunit in the gas phase (Fig. 4*E* and *SI Appendix*, Fig. S8). This observation suggests a weaker interaction between βHb–Hp than αHb–Hp in agreement with the fact that more residues are involved in forming αHb–Hp intermolecular interactions (43). The previous Hp–Hb structural data revealed only the innermost GlcNAc and core fucose residue orientations (42, 43). The highly flexible N-glycan at Asn180 and Asn203 that are close to the Hp–Hb interface, however, may interact with Hb α (αHb)- and/or the β (βHb)-subunit (Fig. 4*A*). Taken together, our results provide a quantitative assessment of the Hb binding events to individual Hp glycoproteoforms and reveal the stabilizing and destabilizing effects on the Hp–Hb complex of N-glycan fucosylation and branching, respectively (Fig. 5).

Discussion

Glycoprotein microheterogeneity arises from the glycan biosynthesis pathway and controls glycoprotein structure and function.
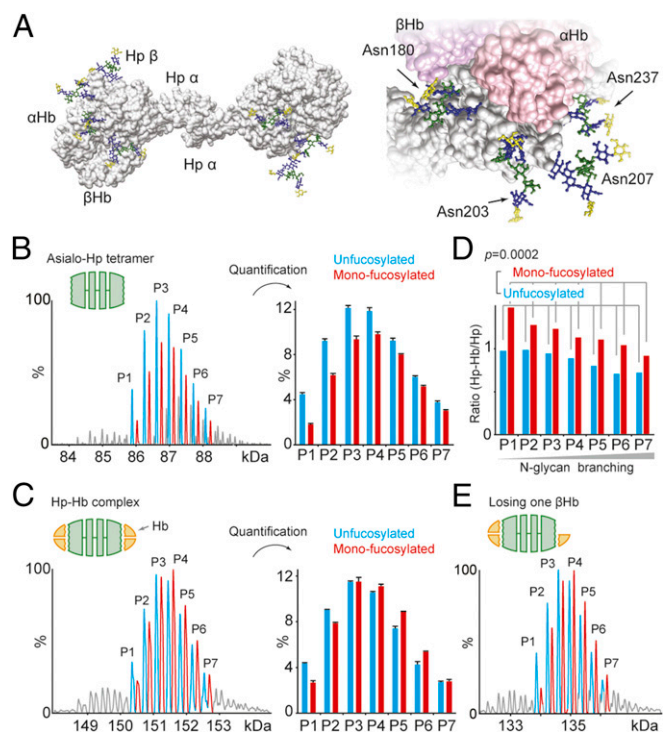
Fig. 4. Native MS analysis of asialo-Hp and Hb interactions. (*A*) Hp–Hb complex structure. The N-glycans on Asn180 and Asn203 are proximal to the Hp–Hb interaction interface. Native mass spectra of asialo-Hp and asialo-Hp–Hb complex (*SI Appendix*, Fig. S6) are deconvoluted to zero-charged spectra (*B* and *C*) using UniDec. The unfucosylated (blue) and monofucosylated (red) peak series of fully glycosylated Hp and the corresponding peak series of Hp–Hb complex with the same glycan compositions are assigned and labeled as P1 to P7. Their relative abundances are extracted and normalized. The ratios of their relative abundances are plotted as bar graph (*D*). Error bars represent the SE of three replicate experiments. (*E*) The spectra of gas-phase dissociated Hp–Hb complexes from which one βHb has been removed.

Wu et al.
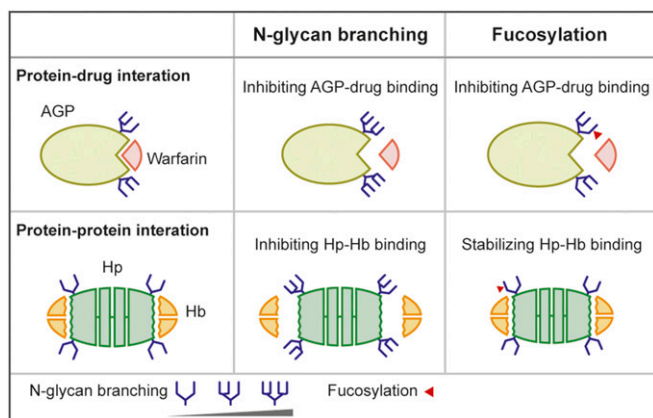
Fig. 5. The schematic illustration of glycosylation regulation of glycoprotein–drug/protein interactions. N-glycan branching and fucosylation may introduce steric hindrance to the warfarin binding pocket inhibiting AGP–drug binding. N-glycan branching attenuates Hp–Hb binding affinity. On the contrary, fucosylation stabilizes the Hp–Hb complex.

Here, we developed high-resolution native MS-based approaches to qualitatively and quantitatively analyze glycoprotein structural microheterogeneity and to define specific functional roles to glycans in modulating drug and protein binding. We demonstrated the global and site-specific microheterogeneity of AGP and Hp. Taking advantage of high-resolution native MS, we identified drug binding to defined asialo-AGP glycoforms and quantified the effects of N-glycan branching and fucosylation on the kinetics of warfarin binding to AGP. We further quantitatively analyzed Hp–Hb complexes and unveiled antagonistic functions of N-glycan branching and fucosylation on Hp–Hb complex stability.

The classic approaches to study glycoprotein–protein interactions are usually based on perturbation of the interaction by removing a target glycan determinant completely, such as glycosyltransferase engineering for N-glycan branching (44) or exoglycosidase digestion for fucosylation (45). However, such perturbations do not address the complexities of the interplay between multiple and heterogeneous occupied N-glycosylation sites. For example, the multiplicity of branched N-glycan gradationally determines the interaction of cell surface receptor kinases with the galectin lattice (46). Here, we demonstrated that N-glycan branching attenuates AGP-warfarin and Hp–Hb interactions in a stepwise manner. Furthermore, our native MS studies of glycoprotein–drug/protein interactions enable us to resolve a protein complex glycoproteoform at the resolution of single monosaccharide residues, and thus assess the subtle effects of glycan fucosylation on protein–drug/protein interactions. Sialylation also plays important roles in regulating protein–protein/ligand interactions (5), and it is feasible that negatively charged terminal sialic acids may introduce extra steric hindrance or interact with the protein backbone, changing glycan orientations in glycoprotein-protein interactions. Although beyond the scope of this study, which focused on asialo-glycoproteins, additional fractionation will be needed to reduce further the complexity of protein glycosylation for future studies by native MS.

From the X-ray crystal structure of recombinant AGP, in which all glycans were removed, it is evident that the N-glycans at Asn-38 and -75 are close to the drug-binding cavity and variable N-glycosylation, especially fucosylation, may modulate access of the cavity to warfarin (17). A previous molecular-dynamics study of AGP revealed that glycosylation expands the volume of the hydrophobic cavity for drug binding (47). Although other glycosylation sites are far from the hydrophobic cavity, the occurrence of distal antennary fucosylation and N-glycan branching/elongation may induce conformational changes to the AGP protein backbone, contributing to a weaker protein–drug interaction. Circulating AGP

is a main drug carrier in the blood and its concentration influences both pharmacokinetics and pharmacodynamics of drug interactions (26). Based on our findings, warfarin binding to AGP is driven by antennary fucosylation and is a crucial consideration for dosage, especially among patients with different secretor and blood group status who have variable degrees of protein fucosylation (48).

Our analysis of the Hp–Hb complex shows N-glycosylation can fine-tune Hp and Hb interactions, even the tight Hp–Hb binding that is widely described as "irreversible," involving over 30 van der Waals and 10 electrostatic interactions (42). For other glycoprotein–protein complexes, N-glycans may have greater effects on their interactions. Fucosylation and N-glycan branching on Hp are both reported to be elevated in various diseases, such as pancreatic (49), hepatic (36), and prostate cancers (50). Based on our results, the Hp glycoproteoforms with higher levels of fucosylation and lower N-glycan branching have greater affinity for Hb. Abnormal Hp in patients therefore may capture the free Hb in blood, delivering it to macrophages more efficiently than normal Hp glycoproteoforms. The N-glycan at Asn-237 is in close proximity to the CD163 binding domain (42). Moreover, N-glycosylations are associated with Hp–Hb complex binding to galectin-1 controlling different endocytic pathways in macrophages (51). Further investigation of fucosylation and N-glycan branching effects on Hp–Hb complex binding to CD163 and galectins may be relevant to understanding both the Hb clearance pathway and disease-specific macrophage activation.

As described above, protein fucosylation is globally regulated and hyperfucosylated glycans on Hp and AGP are elevated in hepatocellular carcinoma (49, 52). Therefore, probing hyperfucosylation on Hp/AGP can provide better clues for identifying and monitoring changes in glycans associated with diseases. More generally, glycoproteins have been widely considered as disease biomarkers; however, the lack of robust and rapid analytical methods to identify glycoprotein-specific changes has limited their implementation (53). While our current study addressed pooled human plasma glycoproteins, we envision that aberrant plasma glycoprotein microheterogeneity, from plasma of individual patients, will be addressable with combined affinity-purifications (54).

Native MS has already shown great prominence in probing protein–drug/ligand binding (55). With this study, we have further demonstrated high-resolution native MS as a powerful platform for pharmacokinetics using complex plasma glycoproteins, subjecting it to minimal sample preparation, and providing drug–protein-binding affinities for each glycoproteoform. The platform is currently unique in that it is able to elucidate the detailed impact of microheterogeneity on drug–protein binding to a glycoprotein, uncovering mechanisms by which subtle changes in N-glycosylation fine-tune the overall protein function. More generally, this approach could be applied to both soluble and membrane proteins to relate changes in ligand binding affinity directly to protein modification status.

Methods

Extended experimental and method details can be found in *SI Appendix*. Human AGP (product number G9885), human Hp phenotype 1-1 (product number H0138), and human Hb (product number H7379) were purchased from Sigma-Aldrich. For native MS analysis, glycoproteins were dissolved in water, buffer exchanged to 200 mM ammonium acetate (pH 7.6), and analyzed on a modified Q-Exactive mass spectrometer (Thermo Fisher Scientific) (56) and a modified Q-Exactive Plus Orbitrap mass spectrometer (57). The raw native MS spectra were deconvoluted using UniDec software to produce zero-charge spectra. Protein and glycan mass calculations were based on amino acid and monosaccharide average residue masses. AGP–warfarin and Hp–Hb binding experiments were performed in ammonium acetate buffer (pH 7.6). Protein structures of AGP [Protein Data Bank (PDB) ID code 3KQ0] (17) and Hp–Hb complex (PDB ID code 4WJG) (43) were retrieved from PDB and processed using University of California, San Francisco Chimera program (version 1.22) (58).

1. Khoury GA, Baliban RC, Floudas CA (2011) Proteome-wide post-translational modification statistics: Frequency analysis and curation of the Swiss-Prot database. *Sci Rep* 1:90.
2. Varki A (1993) Biological roles of oligosaccharides: All of the theories are correct. *Glycobiology* 3:97–130.
3. Dwek RA (1996) Glycobiology: Toward understanding the function of sugars. *Chem Rev* 96:683–720.
4. Varki A (2009) *Essentials of Glycobiology* (Cold Spring Harbor Lab Press, Cold Spring Harbor, NY).
5. Varki A (2017) Biological roles of glycans. *Glycobiology* 27:3–49.
6. Dennis JW, Nabi IR, Demetriou M (2009) Metabolism, cell surface organization, and disease. *Cell* 139:1229–1241.
7. Solá RJ, Griebenow K (2010) Glycosylation of therapeutic proteins: An effective strategy to optimize efficacy. *BioDrugs* 24:9–21.
8. Vuignier K, Schappler J, Veuthey J-L, Carrupt P-A, Martel S (2010) Drug-protein binding: A critical review of analytical tools. *Anal Bioanal Chem* 398:53–66.
9. Yang Y, Barendregt A, Kamerling JP, Heck AJR (2013) Analyzing protein microheterogeneity in chicken ovalbumin by high-resolution native mass spectrometry exposes qualitatively and semi-quantitatively 59 proteoforms. *Anal Chem* 85:12037–12045.
10. Struwe WB, Stuckmann A, Behrens A-J, Pagel K, Crispin M (2017) Global N-glycan site occupancy of HIV-1 gp120 by metabolic engineering and high-resolution intact mass spectrometry. *ACS Chem Biol* 12:357–361.
11. Rosati S, et al. (2013) In-depth qualitative and quantitative analysis of composite glycosylation profiles and other micro-heterogeneity on intact monoclonal antibodies by high-resolution native mass spectrometry using a modified Orbitrap. *MAbs* 5:917–924.
12. Yang Y, et al. (2016) Hybrid mass spectrometry approaches in glycoprotein analysis and their usage in scoring biosimilarity. *Nat Commun* 7:13397.
13. Mehmood S, et al. (2016) Structural and functional basis for lipid synergy on the activity of the antibacterial peptide ABC transporter McjD. *J Biol Chem* 291:21656–21668.
14. Yen HY, et al. (2017) Ligand binding to a G protein-coupled receptor captured in a mass spectrometer. *Sci Adv* 3:e1701016.
15. Taguchi K, Nishi K, Giam Chuang VT, Maruyama T, Otagiri M (2013) *Acute Phase Proteins* (InTech, Rijeka, Croatia).
16. Treuheit MJ, Costello CE, Halsall HB (1992) Analysis of the five glycosylation sites of human α1-acid glycoprotein. *Biochem J* 283:105–112.
17. Schönfeld DL, Ravelli RBG, Mueller U, Skerra A (2008) The 1.8-Å crystal structure of α1-acid glycoprotein (Orosomucoid) solved by UV RIP reveals the broad drug-binding activity of this human plasma lipocalin. *J Mol Biol* 384:393–405.
18. Nishi K, et al. (2011) Structural insights into differences in drug-binding selectivity between two forms of human alpha1-acid glycoprotein genetic variants, the A and F1*S forms. *J Biol Chem* 286:14427–14434.
19. Behan JL, Cruickshank YE, Matthews-Smith G, Bruce M, Smith KD (2013) The glycosylation of AGP and its associations with the binding to methadone. *BioMed Res Int* 2013:108902.
20. Kishino S, et al. (1997) Single-step isolation method for six glycoforms of human alpha1-acid glycoprotein by hydroxylapatite chromatography and study of their binding capacities for disopyramide. *J Chromatogr B Biomed Sci Appl* 703:1–6.
21. Kishino S, et al. (2002) Age- and gender-related differences in carbohydrate concentrations of α1-acid glycoprotein variants and the effects of glycoforms on their drug-binding capacities. *Eur J Clin Pharmacol* 58:621–628.
22. Alayash AI (2011) Haptoglobin: Old protein with new functions. *Clin Chim Acta* 412:493–498.
23. Kristiansen M, et al. (2001) Identification of the haemoglobin scavenger receptor. *Nature* 409:198–201.
24. Spagnuolo MS, Cigliano L, Maresca B, Pugliese CR, Abrescia P (2011) Identification of plasma haptoglobin forms which loosely bind hemoglobin. *Biol Chem* 392:371–376.
25. Urien S, Albengres E, Pinquier JL, Tillement JP (1986) Role of alpha-1 acid glycoprotein, albumin, and nonesterified fatty acids in serum binding of apazone and warfarin. *Clin Pharmacol Ther* 39:683–689.
26. Israili ZH, Dayton PG (2001) Human alpha-1-glycoprotein and its interactions with drugs. *Drug Metab Rev* 33:161–235.
27. Dage JL, Ackermann BL, Halsall HB (1998) Site localization of sialyl Lewis^x antigen on α1-acid glycoprotein by high performance liquid chromatography-electrospray mass spectrometry. *Glycobiology* 8:755–760.
28. Imre T, et al. (2005) Glycosylation site analysis of human alpha-1-acid glycoprotein (AGP) by capillary liquid chromatography-electrospray mass spectrometry. *J Mass Spectrom* 40:1472–1483.
29. Yuasa I, et al. (1997) Human orosomucoid polymorphism: Molecular basis of the three common ORM1 alleles, ORM1*F1, ORM1*F2, and ORM1*S. *Hum Genet* 99:393–398.
30. Yuasa I, et al. (1993) Orosomucoid system: 17 additional orosomucoid variants and proposal for a new nomenclature. *Vox Sang* 64:47–55.
31. Duché J-C, Hervé F, Tillement J-P (1998) Study of the expression of the genetic variants of human α1-acid glycoprotein in healthy subjects using isoelectric focusing and immunoblotting. *J Chromatogr B Biomed Sci Appl* 715:103–109.
32. Lössl P, Snijder J, Heck AJR (2014) Boundaries of mass resolution in native mass spectrometry. *J Am Soc Mass Spectrom* 25:906–917.
33. Marty MT, et al. (2015) Bayesian deconvolution of mass and ion mobility spectra: From binary interactions to polydisperse ensembles. *Anal Chem* 87:4370–4376.
34. Dobryszycka W (1997) Biological functions of haptoglobin—new pieces to an old puzzle. *Eur J Clin Chem Clin Biochem* 35:647–654.
35. Zhang S, Shang S, Li W, Qin X, Liu Y (2016) Insights on N-glycosylation of human haptoglobin and its association with cancers. *Glycobiology* 26:684–692.
36. Zhu J, et al. (2014) Analysis of serum haptoglobin fucosylation in hepatocellular carcinoma and liver cirrhosis of different etiologies. *J Proteome Res* 13:2986–2997.
37. Hülsmeier AJ, Tobler M, Burda P, Hennet T (2016) Glycosylation site occupancy in health, congenital disorder of glycosylation and fatty liver disease. *Sci Rep* 6:33927.
38. Harvey DJ (2005) Fragmentation of negative ions from carbohydrates: Part 1. Use of nitrate and other anionic adducts for the production of negative ion electrospray spectra from N-linked carbohydrates. *J Am Soc Mass Spectrom* 16:622–630.
39. Lee HS, Qi Y, Im W (2015) Effects of N-glycosylation on protein conformation and dynamics: Protein Data Bank analysis and molecular dynamics simulation study. *Sci Rep* 5:8926.
40. Tjernberg A, Markova N, Griffiths WJ, Hallén D (2006) DMSO-related effects in protein characterization. *J Biomol Screen* 11:131–137.
41. Nagel RL, Gibson QH (1971) The binding of hemoglobin to haptoglobin and its relation to subunit dissociation of hemoglobin. *J Biol Chem* 246:69–73.
42. Andersen CBF, et al. (2012) Structure of the haptoglobin-haemoglobin complex. *Nature* 489:456–459.
43. Stødkilde K, Torvund-Jensen M, Moestrup SK, Andersen CBF (2014) Structural basis for trypanosomal haem acquisition and susceptibility to the host innate immune system. *Nat Commun* 5:5487.
44. Guo H-B, Johnson H, Randolph M, Lee I, Pierce M (2009) Knockdown of GnT-Va expression inhibits ligand-induced downregulation of the epidermal growth factor receptor and intracellular signaling by inhibiting receptor endocytosis. *Glycobiology* 19:547–559.
45. Liu Y-C, et al. (2011) Sialylation and fucosylation of epidermal growth factor receptor suppress its dimerization and activation in lung cancer cells. *Proc Natl Acad Sci USA* 108:11332–11337.
46. Lau KS, et al. (2007) Complex N-glycan number and degree of branching cooperate to regulate cell proliferation and differentiation. *Cell* 129:123–134.
47. Fernandes CL, Ligabue-Braun R, Verli H (2015) Structural glycobiology of human α1-acid glycoprotein and its implications for pharmacokinetics and inflammation. *Glycobiology* 25:1125–1133.
48. Albertolle ME, et al. (2015) Mass spectrometry-based analyses showing the effects of secretor and blood group status on salivary N-glycosylation. *Clin Proteomics* 12:29.
49. Pompach P, et al. (2013) Site-specific glycoforms of haptoglobin in liver cirrhosis and hepatocellular carcinoma. *Mol Cell Proteomics* 12:1281–1293.
50. Fujimura T, et al. (2008) Glycosylation status of haptoglobin in sera of patients with prostate cancer *vs*. benign prostate disease or normal subjects. *Int J Cancer* 122:39–49.
51. Carlsson MC, et al. (2011) Galectin-1-binding glycoforms of haptoglobin with altered intracellular trafficking, and increase in metastatic breast cancer patients. *PLoS One* 6:e26560.
52. Tanabe K, Kitagawa K, Kojima N, Iijima S (2016) Multifucosylated alpha-1-acid glycoprotein as a novel marker for hepatocellular carcinoma. *J Proteome Res* 15:2935–2944.
53. Kuzmanov U, Kosanam H, Diamandis EP (2013) The sweet and sour of serological glycoprotein tumor biomarker quantification. *BMC Med* 11:31.
54. Ntai I, et al. (2018) Precise characterization of KRAS4b proteoforms in human colorectal cells and tumors reveals mutation/modification cross-talk. *Proc Natl Acad Sci USA* 115:4140–4145.
55. Pedro L, Quinn RJ (2016) Native mass spectrometry in fragment-based drug discovery. *Molecules* 21:984.
56. Gault J, et al. (2016) High-resolution mass spectrometry of small molecules bound to membrane proteins. *Nat Methods* 13:333–336.
57. van de Waterbeemd M, et al. (2017) High-fidelity mass analysis unveils heterogeneity in intact ribosomal particles. *Nat Methods* 14:283–286.
58. Pettersen EF, et al. (2004) UCSF Chimera—a visualization system for exploratory research and analysis. *J Comput Chem* 25:1605–1612.